ISBN: 978-3-95450-223-3 ISSN: 2673-7000 doi:10.18429/JACoW-NAPAC2019-TUPLM20

GENERATION OF HIGH-CHARGE MAGNETIZED ELECTRON BEAMS CONSISTENT WITH JLEIC ELECTRON COOLING REQUIREMENTS*

A. T. Fetterman, P. Piot[1], Northern Illinois University, DeKalb, IL 60115, USA
S.V. Benson, F. E. Hannon, S. Wang
Thomas Jefferson National Accelerator Laboratory, Newport News, VA 23606, USA
D. Crawford, D. Edstrom, J. Ruan, Fermi National Accelerator Laboratory, Batavia, IL 60510, USA
[1]also at Fermi National Accelerator Laboratory, Batavia, IL 60510, USA

Abstract

The proposed Jefferson Lab Electron-Ion Collider (JLEIC), currently under design, relies on electron cooling in order to achieve the desired luminosity. This includes an electron beam with >55 Mev, 3.2 nC bunches that cools hadron beams with energies up to 100 GeV. To enhance cooling, the electron beam must be magnetized with a specific eigen-emittance partition. This paper explores the use of the Fermilab Accelerator Science and Technology (FAST) facility to demonstrate the generation of an electron beam with parameters consistent with those required in the JLEIC high-energy cooler. We demonstrate via simulations the generation of the required electron-beam parameters and perform a preliminary experiment to validate FAST capabilities to produce such beams.

INTRODUCTION

The Jefferson Laboratory Electron-Ion Collider (JLEIC) is a proposed facility to support experiments in nuclear physics with designed energies for ion or proton of up to 100 GeV. Cooling these beams will require an electron beam with energy >55 MeV [1]. Producing such an electron beam requires a radio-frequency (RF) accelerator. Given the stringent demand on the relative energy spread and beam emittances combined by the 3.2 nC bunch charge, the beam will likely need to be produced with a photoinjector. Lastly, to improve cooling efficiency, the electron beam needs to be magnetized, i.e., have significant canonical angular momentum (CAM).

The specifications for the JLEIC high-energy electron cooler in Table 1 are close to beam parameters attainable at the FAST facility, Fig. 1, at Fermilab. The attainable beam parameters at FAST (either experimentally verified or simulated) match most of the requirements except for the peak-to-peak fractional energy spread which is substantially higher at FAST due to RF-induced curvature on the longitudinal phase space. The uncorrelated fractional energy spread is however comparable to the one required in the JLEIC electron cooling. Thus experiments aimed at exploring the generation of magnetized beams [2] with eigen-emittance partition relevant to JLEIC can be performed at the FAST facility. Magnetized beams have been produced at FAST previously in support for generation of flat beams with high transverse-emittance ratios [3].

* This material is based upon work supported by the U.S. Department of Energy, Office of Science and the Office of Nuclear physics under contracts DE-AC05-06OR23177 and DE-AC02-07CH11359.

Table 1: Comparison for the electron-cooling beam requirements for the JLEIC parameters [1] and corresponding value (inferred from simulations) achievable at FAST. All values are RMS quantities and the emittances are normalized.

Parameter	Unit	JLEIC	FAST
Beam Energy	MeV	[20,55]	45
Beam Charge	nC	3.2	>3.2
cath. spot size	mm	1.1	1
B field on cath.	T	0.05	< 0.09
cyclotron emitt.	μm	≤ 19	< 5
drift emitt.	μm	36	37
δp/p (uncor.)	-	3.10^{-4}	$< 4.10^{-4}$
δp/p (pk-to-pk.)	-	$<6.10^{-4}$	$O(10^{-4})$
bunch length σ_z	cm	2	0.2

GENERATION & ACCELERATION OF MAGNETIZED BUNCHES AT FAST

The magnetization sets the eigen-emittance partition that can ideally be achieved. It is given by $\gamma\mathcal{L} = \frac{eB_c}{2mc}\sigma_c^2$, where we refer to $\gamma\mathcal{L}$ as the *normalized* magnetization. B_c is the axial magnetic field on the photocathode surface and σ_c the rms transverse size (assumed to be identical within the two transverse directions). Here we should note that $\gamma\mathcal{L}$ plays the role of an emittance and the effective emittance associated with a beam with significant CAM is $\varepsilon_{n,\text{eff}} = [(\gamma\mathcal{L})^2+\varepsilon_{n,u}^2]^{1/2}$. Assuming a CAM-dominated beam $\gamma\mathcal{L} \gg \varepsilon_{n,u}$ the eigen-emittances $\varepsilon_{n,\pm}$ are given by

$$\varepsilon_{n,+} = 2\gamma\mathcal{L} \equiv \varepsilon_{n,d} \text{ and } \varepsilon_{n,-} = \frac{\varepsilon_{n,u}^2}{2\gamma\mathcal{L}} \equiv \varepsilon_{n,c} \qquad (1)$$

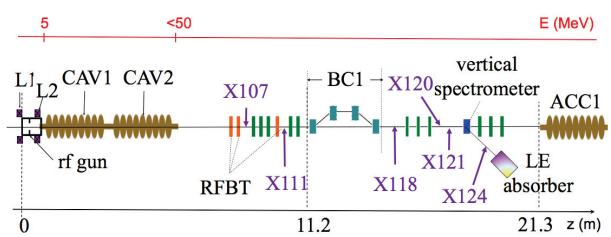

Figure 1: Layout of the FAST injector. The red quads labeled RFBT are the skew quads that form the transformation lattice for the conversion of round magnetized beam to flat beams.

ISBN: 978-3-95450-223-3 ISSN: 2673-7000 doi:10.18429/JACoW-NAPAC2019-TUPLM20

where $\varepsilon_{n,u}$ refers to the intrinsic (thermal) emittance, $\varepsilon_{n,d}$ and $\varepsilon_{n,c}$ are respectively referred to as the normalized drift and cyclotron (or Larmor) emittances. Note that the eigen-emittances ε_m (with $m \equiv \pm$) can formally be obtained from the 4×4 beam matrix by solving the characteristic equation $\det[J\Sigma^{-1} - i\varepsilon_m I] = 0$ where I and J are respectively the identity and unitary symplectic matrix.

The settings of the FAST injector were optimized using ASTRA employing an axisymmetric $r - z$ space charge algorithm [4]. The optimizations were performed using a multi-objective non-dominated sorting technique. The laser spots size and peak field of the bucking and main solenoids were variables in the optimization process. The other beamline settings (cavity phase and field and photocathode-laser settings) were set to conservative values corresponding to FAST nominal operating point. The two main objectives were to

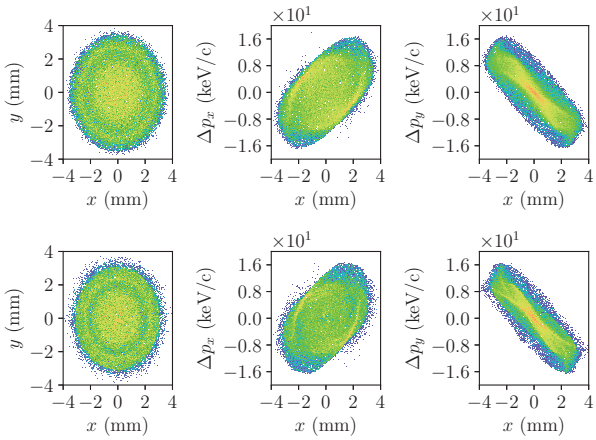

Figure 2: Comparison of beam transverse distribution (left column), horizontal phase space (middle column) and $x - p_y$ distribution (right column) simulated with ASTRA (upper row) and IMPACT-T (lower row). The distributions are taken at $z = 8$ m from the photocathode.

produce a magnetized beam with drift emittance around $\varepsilon_{n,d} = 36$ μm while minimizing the four-dimensional emittance defined as $\varepsilon_{n,4D} \equiv (\varepsilon_{n,d}\varepsilon_{n,c})^{1/2}$. Figure 3 shows an example of beam emittances evolution along the FAST photoinjector with final eigenemittance partition fulfilling the JLEIC requirements. The ASTRA simulations were also validated against IMPACT-T 3-D space-charge algorithm [5]. Figure 2 shows the fidelity of the two codes.

MEASURING DRIFT & CYCLOTRON EMITTANCES

Conversion of Magnetized Beam into Flat Beam

Decoupling of a cylindrical-symmetric magnetized beam into a flat beam is well established [6]. The FAST injector includes three skew quadrupole magnets (Q106, Q107, Q111 in Fig. 1) which can decouple the beam and produce a flat beam [7]. In the process, the eigen-emittances are ideally mapped into conventional emittances along the

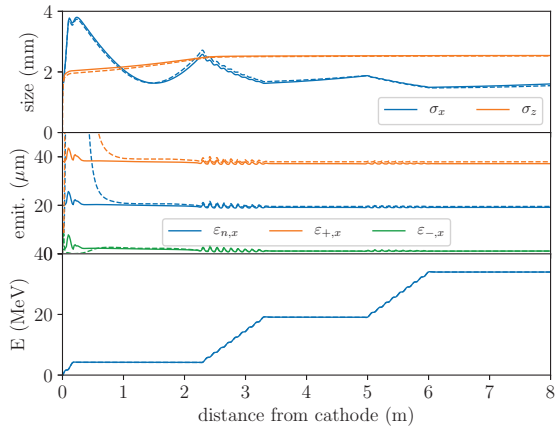

Figure 3: Comparison of rms beam size (top row), rms emittances (middle row) and total energy (lower row) simulated with ASTRA (solid traces) and IMPACT-T (dashed traces).

horizontal and vertical degrees of freedom. This round-to-flat-beam transformer (RFBT) can be used to verify that the eigen-emittances produced by the injector have value relevant to the JLEIC electron-cooling project. Downstream of the RFBT several quadrupole magnets can be used to transport the beam up to an upstream multi-slit emittance station (located at X118). In the simulations, the following

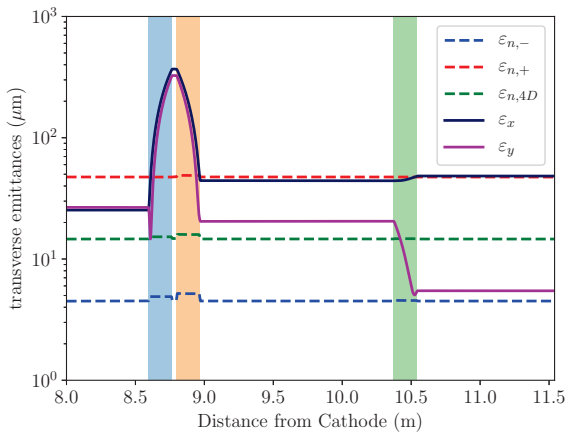

Figure 4: Impact-T simulations of the transfer of the eigen emittances (dotted lines) to the conventional emittances (solid lines). The shaded vertical rectangles indicate the locations of the skewed quadrupole magnets.

procedure is used to decouple the beam and transform it into a flat beam. The correlation matrix is computed at $z = 8$ m from the photocathode using the macroparticle phase-space distribution. The correlation matrix is used to compute the skew-quadrupole magnet settings using the formulae derived in [8] under the thin-lens approximation. The analytically-computed values are used as a starting point in the ELEGANT optimizer to further tune the quadrupole settings (taking into account the thick-lens model) to realize an uncoupled beam

ISBN: 978-3-95450-223-3 ISSN: 2673-7000 doi:10.18429/JACoW-NAPAC2019-TUPLM20

downstream of the RFBT. A single-objective optimization target function $\chi \equiv |\Sigma_{13}| + |\Sigma_{14}| + |\Sigma_{23}| + |\Sigma_{24}|$ is introduced. Finally, the optimized quadrupole-magnet strength are then loaded in IMPACT-T where further optimization can be made while accounting for space charge effects; see Fig. 4.

Measuring Emittances of the Magnetized Beam

Using a scanning slit to intercept the magnetized beam and analyzing the transmitted beamlets provide the correlated and uncorrelated emittances which are indirectly related to the eigen-emittances [2]. An example of simulations

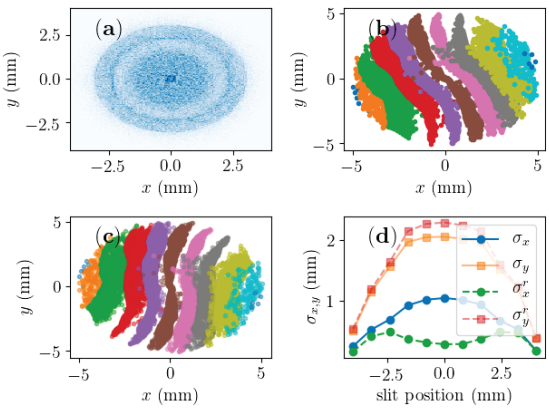

Figure 5: Simulation of the scanning slit measurement. Initial magnetized beam distribution (a), beamlet image after the scanning slit before (b) and after (c) removal of mean rotation angle, and (d) corresponding beamlet sizes [the subscripts r indicate beamlet size computed from data shown in (c)]. In (b) and (c) each color correspond to a slit positions.

illustrating the method appears in Fig. 5. A scanning slit was simulated and the set of transmitted beamlets was used to infer the correlated emittance Fig. 5(b) while the same set of data was processed to remove the mean rotation angle and to infer the uncorrelated emittance. For the simulated example (corresponding to Fig. 3) we find the retrieve correlated and uncorrelated emittance to be respectively $\gamma\mathcal{L} = 19.4$ µm and $\gamma\varepsilon_{n,u} = 7.8$ µm. These values yield an indirectly measured eigen-emittance partition of $(\varepsilon_{n,-}, \varepsilon_{n,+}) = (1.6, 38.8)$ µm in reasonable agreement with the simulated emittance partition is (1.1, 37.9) μm.

PRELIMINARY MEASUREMENTS

A series of preliminary experiments were performed during the spring 2019 run of FAST. The experiments focused on producing the required bunch charge and magnetization and attempted to measure the beam emittance using the available RFTB, see Fig. 6. A bunch charge of 3.2 nC was produced Fig. 6(a) and a set of data was collected for $B_{cath} \simeq 660$ G. The beam was transformed into a flat beam using the RFBT, Fig. 6(d), with associated emittances of 2±1 μm and 32±3 μm. The beam-emittance measurement was performed using the multi-slit technique and was limited by the dynamical range in emittance (e.g. overlap of the beamlets originating from the different slits). The diagnostics limitations were addressed during the summer shutdown and a scanning slit scheme was implemented. It should be noted that the eigen-emittances inferred from the magnetized-beam emittance measurement were found to be 75±3 μm and 0.5±1 μm. The large observed discrepancy is partially attributed to the limited beam quality (the photocathode distribution on the cathode could not be made uniform as seen in Fig. 6(b).

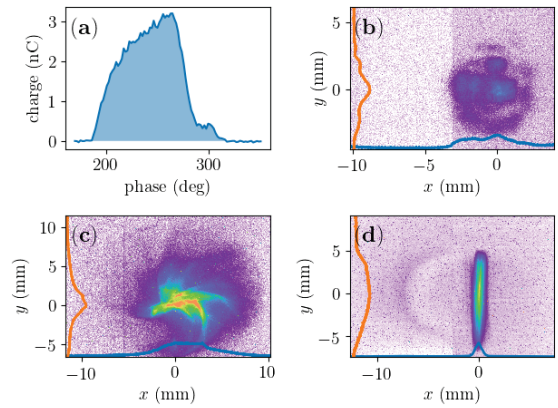

Figure 6: Example of measurements. Bunch charge as a function of laser launch phase (a), laser distribution on the photocathode surface (b), magnetized-beam distribution at X109 (c), and at X118 downstream of the RFTB (d).

Table 2: Measurements of the cathode spot size, magnetic field on the cathode and the momentum of the beam in the axial direction along with expected emittance measurements.

Parameters	Measurements
Magnetic field (Tesla)	0.0665±.0005
Beam Spot Size (mm)	1.448±.004
Momentum (MeV/c)	32.436±.001
Emittance	**Calculations**
Magnetization $\mathcal{L}$ (μm)	41.5±3
Drift emit., $\epsilon_{n,+}$ (μm)	83±6
Cyclotron emit., $\epsilon_{n,-}$ (μm)	2.3±0.3
Emittance	**Measurements**
Magnetization $\mathcal{L}$ (μm)	31.2±1.1
$\epsilon_{n,+}$ (μm)	62.4±2.2
$\epsilon_{n,-}$ (μm)	3±0.8

The simulated magnetization and eigen emittances are compared with the measured ones in Table 2. The data and simulations agree within 30% and we expect the next round of experiment (with improved diagnostics and laser system) will enable better measurements. The next round of experiment will also focus on transporting the magnetized beam over longer distances to explore possible degradation of eigen emittances.

ISBN: 978-3-95450-223-3 ISSN: 2673-7000 doi:10.18429/JACoW-NAPAC2019-TUPLM20

REFERENCES

[1] S. Benson *et al.*, "Development of a Bunched Beam Electron Cooler Based on ERL and Circulator Ring Technology for the Jefferson Lab Electron-Ion Collider," in *Proceedings, International Workshop on Beam Cooling and Related Topics (COOL'17)*, Bonn, Germany, September 18-22, 2017, paper WEM12, pp. 72-76.

[2] Y.-E. Sun, P. Piot, K.-J. Kim, N. Barov, S. Lidia, J. Santucci, R. Tikhoplav, and J. Wennerberg, "Generation of angular-momentum-dominated electron beams from a photoinjector," *Phys. Rev. ST Accel. Beams*, vol. 7, p. 123501, Dec 2004.

[3] A. Halavanau, P. Piot, D. Edstrom, A. Romanov, D. Crawford, J. Ruan, D. Mithalcea, V. Shiltsev, and S. Nagaitsev, "Magnetized and flat beam generation at the fermilab's fast facility," in *Proceedings, 9th International Particle Accelerator Conference (IPAC 2018),* Vancouver, BC Canada, April 29-May 4, p. THPAK061, 2018.

[4] K. Flöttman, "A space charge tracking algorithm ASTRA," *user manual*, 2017.

[5] J. Qiang, S. Lidia, R. D. Ryne, and C. Limborg-Deprey, "Three-dimensional quasistatic model for high brightness beam dynamics simulation," *Phys. Rev. ST Accel. Beams*, vol. 9, p. 044204, Apr 2006.

[6] K.-J. Kim, "Round-to-flat transformation of angular-momentum-dominated beams," *Phys. Rev. ST Accel. Beams*, vol. 6, p. 104002, Oct 2003.

[7] J. Zhu, P. Piot, D. Mihalcea, and C. R. Prokop, "Formation of compressed flat electron beams with high transverse-emittance ratios," *Phys. Rev. ST Accel. Beams*, vol. 17, p. 084401, Aug 2014.

[8] E. Thrane *et al.*, "Photoinjector Production of A Flat Electron Beam," in *Proc. 21st Linear Accelerator Conf. (LINAC'02), Gyeongju, Korea, Aug. 2002*, p. 308, 2002.